

Molecular Dynamics Simulations of the Bis-Intercalated Complexes of Ditercalinium and Flexi-Di with the Hexanucleotide d(GCGCGC)₂: Theoretical Analysis of the Interaction and Rationale for the Sequence Binding Specificity

Beatriz de Pascual-Teresa,[§] José Gallego,[†] Angel R. Ortiz,[‡] and Federico Gago*

Departamento de Fisiología y Farmacología, Universidad de Alcalá, E-28871 Alcalá de Henares, Madrid, Spain

Received June 10, 1996[⊗]

The X-ray crystal structures of the complexes of ditercalinium and Flexi-Di with d(CGCG)₂ have been studied by computational chemistry methods in an attempt to rationalize their distinct structural features. In addition, the complexes of these two bisintercalating drugs with d(GCGCGC)₂ have been modeled and subjected to 0.5 ns of molecular dynamics simulations in explicit solvent with the aim of evaluating the relative importance of hydrogen bonding and stacking interactions in the sequence binding specificity of these compounds. According to our calculations, the electrostatic term is *attractive* for the stacking interactions between the pyridocarbazole chromophores of these drugs and the base pairs that make up the sandwiched GpC step. On the contrary, this energy term is *repulsive* for the base pairs that make up the boundaries of the bisintercalation site. This differential electrostatic binding energy component, which is shown to have a strong orientational dependence, could lie at the origin of the observed binding preferences of these drugs. In addition, both the Lennard–Jones and the electrostatic energy terms contribute to stabilizing the underwound central GpC step. The attractive electrostatic interactions between the linkers and the major groove are in concert with the stacking specificities for the sandwiched GpC step, which is thus very effectively stapled by the drugs. The hydrogen-bonding potential of the linkers, however, appears to be reduced in an aqueous medium due to competing interactions with water. Binding of either ditercalinium or Flexi-Di to d(GCGCGC)₂ appears to favor the A-type conformation that this DNA molecule most likely adopts in the free state. The possible relevance of these findings to the process of bis-intercalation and to the pharmacological action of these compounds is discussed.

Introduction

Ditercalinium (Figure 1a) is a bifunctional intercalating molecule with antitumor activity which binds to DNA preferentially at GC-rich regions.¹ Dimerization of the chromophore was aimed at increasing the binding affinity, and the central linker was selected to prevent the intramolecular stacking of the two aromatic rings and to increase the lifetime of the complex by hampering the displacement of the ligand along the DNA helix.² Besides, the amino alkyl chain increases the water solubility of the dimers and enhances the DNA affinity through electrostatic interactions. As a matter of fact, ditercalinium dissociates from d(CGCG)₂ about 100–1000 times more slowly than the corresponding monomer.³ Other dimers with one, two or three additional methylene groups between the two piperidine rings also bis-intercalate, and their affinities are even higher than that of ditercalinium. However, the cytotoxicity of these compounds, which has been mainly related to a lethal drug-induced DNA deformation,⁴ is drastically reduced when the number of methylenes is greater than one.⁵ A structural analogue of ditercalinium containing a very flexible spacer with the same number of atoms separating the two chromophores and equal net charge (Flexi-Di, Figure 1b), has been found to be devoid of pharma-

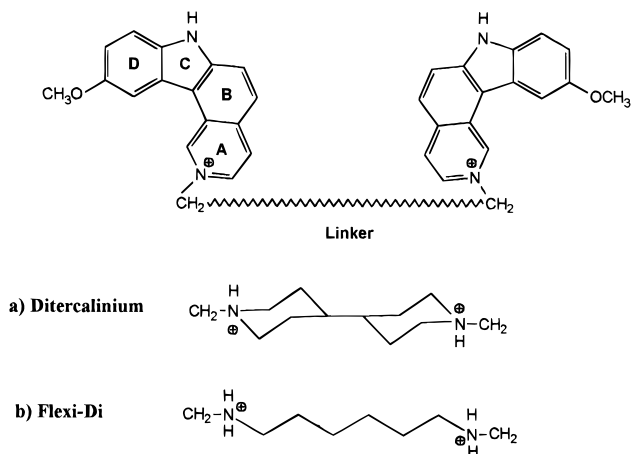


Figure 1. Chemical structures of ditercalinium (a) and Flexi-Di (b).

cological activity in eukaryotic cells, even though it also behaves as a true bis-intercalator.⁶ Interestingly, other ditercalinium analogues containing linking chains attached to any other position of the chromophore or having different net charge, length or flexibility, have also been shown to lose the antitumor potency of the parent compound even though many of them still retain the same bisintercalating properties.^{7,8} Thus, there appears to be no direct correlation between DNA binding affinity and antitumor activity.²

In order to understand the structural alterations of the DNA molecule brought about by the reversible binding of ditercalinium and analogues, a great deal of work has been carried out. The pioneering ¹H- and ³¹P-

* Author to whom correspondence should be addressed.

[†] Present address: Department of Chemistry, University of Washington, Seattle, WA 98195.

[‡] Present address: The Scripps Research Institute, La Jolla, CA 92037.

[§] Present address: Departamento de Química, Universidad San Pablo CEU, 28668 Madrid.

[⊗] Abstract published in *Advance ACS Abstracts*, November 1, 1996.

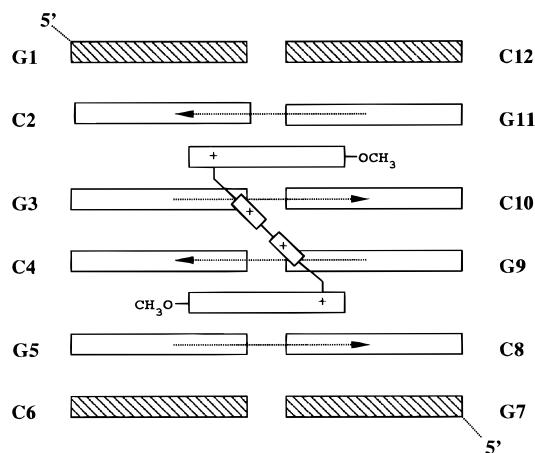


Figure 2. Schematic view from the major groove of a complex between ditercalinium or Flexi-Di and a DNA hexamer containing a central GpC binding site. The + signs highlight positively charged fragments. Dipole moment vectors for the base pairs are represented as arrows.

NMR studies of Roques and co-workers^{3,6,9,10} showed that each pyridocarbazolium ring of ditercalinium was able to intercalate into each of the contiguous CpG steps of a $d(\text{CGCG})_2$ oligonucleotide. In contrast, binding of ditercalinium to $d(\text{GCGC})_2$ showed one ring of the drug intercalated at the CpG step and the other stacked on top of either of the external base pairs.¹¹ In both cases, however, the convex edge of the chromophores was oriented toward the minor groove. This orientation places the linker diagonally across the major groove and ensures that the chromophores adopt antiparallel orientations relative to each other, which confers the molecule an inverted-Z shape when seen from the major groove (Figure 2). The proton spectra of the complexes of ditercalinium with $d(\text{TTCGCGAA})_2$ and $d(\text{CGCG})_2$ are very similar,⁶ and both retain 2-fold symmetry. On the other hand, binding of ditercalinium to $d(\text{CCTATAGG})_2$ does not lead to a unique complex and extensive line broadening is observed, indicative of nonspecific binding despite the alternation of 5'-Pyr-Pur-3' in the central region.¹¹

The preference for intercalation at 5'-CpG-3' steps of the majority of monointercalators (with one notable exception in actinomycin D, which binds to a GpC step)¹² is supported by ample experimental evidence¹³⁻¹⁵ and was not unexpected for ditercalinium. This preference is generally attributed to the lower energy required for unstacking this sequence relative to others.¹⁶⁻¹⁸ It is not clear, however, why ditercalinium dislikes the GpC step for intercalation¹¹ or why, in common with other 6*H*-pyridocarbazole-containing compounds,¹⁹ the indole nitrogen of the chromophore always points toward the DNA minor groove. Though it has been suggested that the bis(ethylpiperidinium) linker could be fundamental in dictating the groove preference of ditercalinium,¹¹ examples are known of similar linking chains found in the minor groove of TpA steps.²⁰ In any case, this functionality does not seem adequate to detect base pair reversals (*e.g.* GpC vs CpG) given that the N7 and O6 atoms of the guanines lie diagonally across the major groove in both steps.

Finer details of the structure of a ditercalinium- $d(\text{CGCG})_2$ complex have been obtained by means of X-ray crystallographic studies.^{21,22} Among the most remarkable features found are (1) complete lack of van

der Waals contacts between the bases of the terminal cytidines and the chromophores of ditercalinium; (2) poor stacking of the drug's chromophore on the internal cytosines; (3) lack of 2-fold symmetry in the conformation and interactions of the two halves of the complex; (4) lack of van der Waals contacts between the cytosines and the bis(ethylpiperidinium) linker, which can form only one hydrogen bond with the DNA major groove; and (5) significant bending of the DNA helical axis toward the minor groove ($\sim 15^\circ$ kink).

In the light of this crystal structure it was reasoned that this unusual deformation of the DNA could arise from the limited flexibility of the linker.²² It came then as a surprise that the crystal structure of the same DNA sequence complexed with Flexi-Di revealed many similar features and an even higher degree of bending.²³ Since the orientation of the *N,N*-diethyl-1,6-hexanediammonium linker of Flexi-Di increases the hydrogen bonding potential of this linker over that of the more rigid bis(ethylpiperidinium) spacer of ditercalinium, it was proposed that DNA bending originates in these complexes by a concerted *push/pull* effect mechanism involving specific hydrogen bonding and base pair-chromophore stacking interactions.²³

We thought it would be of considerable interest to analyze these stacking interactions in detail because we have previously shown their relative importance in determining binding specificity²⁴ and dictating DNA conformational preferences^{25,26} in other bis-intercalator-DNA complexes. We were also interested in probing, by simulation methods, to what extent the amount and the direction of bending could be influenced by lattice forces and by the presence of surrounding complexes in the crystal, which must surely give rise to a very different electrostatic environment from that of the complex in aqueous solution. Finally, we wanted to assess the possible perturbations inflicted on the DNA upon bis-intercalation over slightly longer distances (*i.e.* beyond first neighbors) in a dynamical context.

In our attempt to shed light on these issues, we constructed computer models of the complexes of ditercalinium and Flexi-Di with the alternating hexanucleotide $d(\text{GCGCGC})_2$, in which each drug embraces the central GpC binding site (Figure 2). The complexes were fully solvated and neutralized by addition of sodium counterions, and dynamics simulations were run for 500 ps. For comparison purposes, two additional simulations were performed, in which the charges of the linkers were "switched off".

Methodology

(1) Model Building and Energy Refinement. The X-ray crystal structures of the complexes between $d(\text{CGCG})_2$ and ditercalinium (1.7 Å resolution, *R*-factor = 22.5%),²¹ and between $d(\text{CGCG})_2$ and Flexi-Di (2.5 Å resolution, *R*-factor = 23.9%)²³ were retrieved from the Brookhaven Data Bank.²⁷ Hydrogen atoms were added to the molecules using standard geometries. In order to achieve electrical neutrality, four counterions resembling hexahydrated sodium ions were placed in the bisector of the O-P-O groups located further from the positively charged ligand.²⁸

The all-atom AMBER molecular mechanics force field^{29,30} was used throughout. Consistent parameters were derived³¹ to describe the bonded and nonbonded interactions involving drug atoms (Supporting Information, item 1). For the 1-methyl-10-methoxy-7*H*-pyrido[4,3-*c*]carbazolium chromophore and the bis(methylpiperidinium) and *N,N*-dimethyl-1,6-hexanediammonium linkers, molecular electrostatic potentials (MEPs)

were calculated from the corresponding *ab initio* wave functions (6-31G⁺/STO-3G). Partial atomic charges (Supporting Information, items 2–4) were then derived by fitting each MEP to a monopole–monopole expression.^{32,33} Point charges for the linker atoms were set to zero in the simulations where the electrostatic term for the linkers was “switched off”.

Both molecular systems were adapted to AMBER by progressively minimizing their potential energy: first, only the counterions and hydrogen atoms were allowed to move; second, the interactions between the drug linkers and the central base pairs were optimized; and, finally, the whole systems were relaxed. Before each minimization stage, a short optimization run restraining the atoms to their initial coordinates allowed readjustment of covalent bonds and van der Waals contacts without changing the overall conformation of the complexes. All atom pairs were included in the calculation of the non-bonded interactions, and the solvent environment was simulated by performing the optimizations in a continuum medium of relative permittivity $\epsilon = 4r_{ij}$. For the first 3000 steps of the global minimization, all hydrogen bonds between the DNA base pairs were reinforced with distance and angle restraining functions with force constants of 10 kcal mol⁻¹ Å⁻² and 10 kcal mol⁻¹ rad⁻², respectively. The optimizations covered a total of about 6000 steps of steepest descent energy minimization for each of the complexes.

These preliminary molecular mechanics calculations showed the linkers to be highly strained, and subsequent molecular dynamics simulations in water using the reported geometries for the linkers proved unstable, with a strong tendency of one of the chromophores to stick out of the complexes. It has been pointed out that, at the intermediate resolution of most drug–DNA analyses, errors may persist during crystallographic refinement due to the bias imposed by the model that is built into it even in cases where the residual error is acceptable.^{34,35} In the case of the ditercalinium complex, initial difficulties for solving the structure by molecular replacement were precisely due to a wrong positioning of the linker, and the crystal was later found to diffract to only 2.5 Å resolution in the cell direction approximately perpendicular to the DNA helical axis.²¹ The Flexi-Di linker is reported to have been constructed from coordinates of a spermine molecule and added to the model,²³ this fact, together with the intermediate resolution of this crystal structure, precludes the accurate location of the linker atoms, which nevertheless are highly disordered. We thus felt it was justified to reoptimize the geometry of both linkers. To this end, 1-ns high-temperature restrained molecular dynamics simulations were undertaken in order to find a more suitable starting conformation for the linking chains. The temperature was gradually raised to 300 K, then to 600 K, and finally to 900 K during the first 15 ps. All atoms, except those connecting the two chromophores, were restrained to their reference positions in cartesian space using a harmonic force constant of 100 kcal mol⁻¹ Å⁻². After another 15 ps of equilibration, system coordinates were saved every 0.1 ps for the remaining 970 ps at 900 K. The time step used was 1 fs during the heating period and 2 fs during the rest of the simulations. All bonds involving hydrogens were constrained to their equilibrium values by means of the SHAKE algorithm,³⁶ and the lists of nonbonded pairs were updated every 25 steps. The interaction energies between each ligand and the DNA molecules were monitored and analyzed along the dynamics simulations using a $4r_{ij}$ dielectric constant and a cutoff of 10 Å for the nonbonded interactions. The 10 lowest energy conformations were then selected and energy minimized. After minimization, most of the selected low-energy conformations for each molecule converged to a unique conformation, which was energy minimized as above and analyzed (Table 1). The root-mean-square deviation (rmsd) with respect to the corresponding X-ray coordinates, for all non-hydrogen atoms of the bound ligands, was 0.4 Å for ditercalinium and 0.6 Å for Flexi-Di (Figure 3).

These energy-minimized structures were used as templates for the generation of the complexes of each of these drugs with a double-stranded alternating hexamer containing three contiguous GpC sites, of which the central one is sandwiched by the drug chromophores (Figure 2). We chose to represent a

Table 1. Decomposition of the Electrostatic (ele) and Lennard–Jones (LJ) Interaction Energies between the Drugs' Chromophores and Individual Base Pairs and between the Linkers and the DNA Molecule

| DNA Molecule | d(CGCG) ₂ –ditercalinium | | | | | | | | | | d(CGCG) ₂ –Flexi-Di | | | | | | | | | | | | | |
|----------------|-------------------------------------|-------|-------|-------|--------|------------------|-------|--------|-------|-------|--------------------------------|-------|-------|--------|-------|----------------|--------|-------|-------|--------|-------|-------|--------|-------|
| | X-ray | | | | | modeled, refined | | | | | X-ray | | | | | X-ray, refined | | | | | | | | |
| | ele | | ele | | | ele | | | ele | | | ele | | ele | | | ele | | ele | | | | | |
| D ^a | A ^b | LJ | D | A | LJ | D | A | LJ | D | A | LJ | D | A | LJ | D | A | LJ | D | A | LJ | D | A | LJ | |
| C2:G11 | 0.29 | 1.9 | -19.1 | -0.09 | 0.7 | -19.4 | -0.12 | 1.1 | -19.8 | 0.43 | 2.1 | -19.2 | 0.10 | 1.9 | -19.0 | 0.16 | 2.1 | -19.4 | 0.16 | 2.1 | -19.0 | 0.16 | 2.1 | -19.4 |
| G3:C10 | -0.99 | -6.3 | -20.0 | -0.45 | -5.0 | -19.5 | -0.76 | -5.3 | -19.8 | -0.80 | -6.4 | -20.2 | -0.68 | -5.8 | -20.6 | -0.87 | -6.1 | -20.4 | -0.87 | -6.1 | -20.6 | -0.87 | -6.1 | -20.4 |
| C4:G9 | -1.41 | -7.6 | -20.4 | -1.29 | -6.9 | -20.6 | -1.35 | -6.9 | -20.5 | -0.84 | -7.0 | -18.2 | -0.88 | -6.5 | -17.6 | -0.90 | -6.7 | -17.5 | -0.90 | -6.7 | -17.6 | -0.90 | -6.7 | -17.5 |
| G5:C8 | 0.38 | -1.8 | -18.7 | 0.09 | 1.0 | -19.2 | 1.17 | 1.5 | -19.2 | 0.32 | 2.7 | -15.4 | 0.12 | 1.9 | -15.0 | 0.17 | 1.8 | -15.1 | 0.17 | 1.8 | -15.0 | 0.17 | 1.8 | -15.1 |
| linker | -4.62 | -58.5 | 63.9 | -4.50 | -157.6 | -9.8 | -6.34 | -166.2 | -10.6 | -8.16 | -142.6 | 5.5 | -7.69 | -168.6 | -8.3 | -9.48 | -174.1 | -8.3 | -9.48 | -174.1 | -8.3 | -9.48 | -174.1 | -8.3 |

^a Calculated by solving the Poisson–Boltzmann equation. ^b Calculated with AMBER and a dielectric constant of 1.

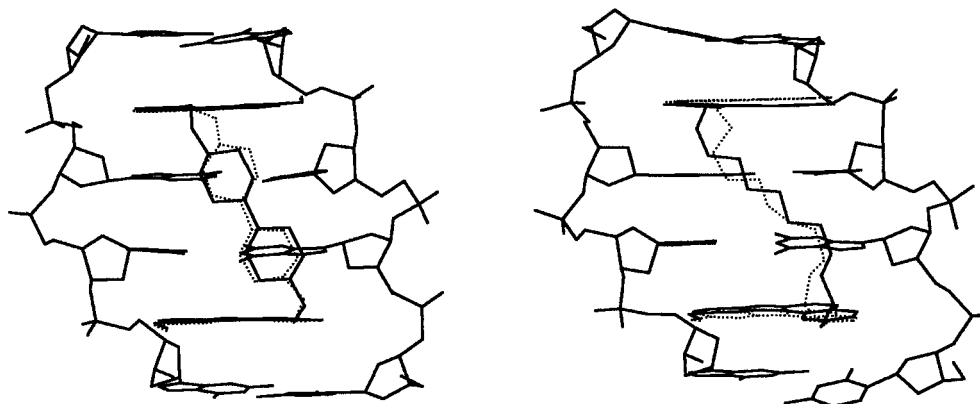


Figure 3. View down the major groove of the complexes between d(CGCG)₂ and either ditercalinium (left) or Flexi-Di (right) as reported in the X-ray crystal structures (dotted lines) and after remodeling of the linking chains (thick lines).

section of a slightly longer DNA fragment in an attempt to better assess the extent of helix deformation for longer sequences and minimize the possibility of end effects affecting the central region during the dynamics simulations in water. In order to add a terminal G:C base pair on both 5'- and 3'-ends, a symmetry related copy was generated on each side of the helix by applying the appropriate symmetry operators as the complexes are aligned with the 5'-ends of a given strand stacked over the 3'-end of the adjacent strand so that infinite helices are formed in the crystal lattice.^{21–23} The advantages of this procedure are that the stacking interactions are already optimized and that it is relatively easy to add the extra bridging phosphate in a suitable geometry. A short optimization run restraining the ligand and base atoms to their initial coordinates allowed readjustment of the sugar–phosphate backbone while maintaining the overall conformation of the complexes.

These extended complexes were then placed in the center of rectangular boxes with dimensions such that the minimum distance between any atom in the complexes and the wall of the boxes was 8 Å. The boxes were immersed into a Monte Carlo-equilibrated configuration of TIP3P water molecules,³⁷ and any water molecules outside the box or whose oxygen or hydrogen atoms lay within 2 or 1 Å, respectively, of any DNA or ligand atom were removed. This procedure yielded systems with 1744 and 1681 water molecules for the ditercalinium–d(CGCGCG)₂ and Flexi-Di–d(CGCGCG)₂ models, respectively, on which periodic boundary conditions were applied.

The water molecules were allowed to optimize their interactions with the complexes by subjecting them to 500 steps of steepest-descent energy minimization followed by 6 ps of molecular dynamics at 300 K and further energy minimization for another 500 steps. The whole systems were then relaxed by performing 3000 steps of steepest-descent energy minimization. In order to achieve electrical neutrality, six sodium ions³⁸ (or eight in the simulations with uncharged linkers) were included in each system following the procedure described in the next section.

(2) Electrostatic Energy Calculations and Location of the Counterions. Most molecular mechanics force fields describe the energy of interaction between two charged systems *i* and *j* embedded in a medium of relative dielectric constant ϵ by means of a Coulombic term of the form:

$$E_{\text{el(MM)}} = \sum_{ij} \frac{q_i q_j}{\epsilon r_{ij}}$$

where *q* represents partial atomic charges and *r* is the separation between any two of them. When one is interested in calculating electrostatic interaction energies for complexes in solution, the above expression may not be accurate enough as it does not take into account the dielectric discontinuity between the low dielectric solute and the high dielectric solvent.³⁹ It then becomes essential to assign a proper value to ϵ . Continuum electrostatics based on the Poisson–Boltz-

mann equation⁴⁰ can explicitly account for the different polarizabilities of both the DNA–ligand complex and the solvent around it. Numerical solutions to this equation were obtained by using the finite difference method implemented in the DelPhi module of Insight-II.⁴¹ To this end, a grid (0.8 Å/grid point) was superimposed on the molecular systems considered, and the electrostatic potential was calculated at each point. The solvent-accessible surface of the complex,⁴² calculated with a spherical probe of 1.4 Å radius, was used to define the boundary of the low dielectric medium ($\epsilon = 2$) in which the solute charges are embedded. The surrounding solvent was treated as a continuum of dielectric constant 80. The ion exclusion radius for the Stern layers was 2 Å. The ionic strength was calculated according to the number of sodium ions present in each box of water and set to average values of 0.195 and 0.260 mol/L for the simulations with charged and uncharged linkers, respectively.

Electrostatic interaction energies between any two groups of atoms *i* and *j*, e.g. the chromophore and one of the adjacent base pairs, were calculated by computation of the potential at each of the atoms of group *j* due to the charges on all of the atoms of group *i* (ϕ_j) and summation over all of the atoms in group *j*:⁴³

$$E_{\text{el(PB)}} = \sum_j \phi_j q_j$$

The potential at the location of each atom was obtained by interpolation from the potentials at the surrounding grid points, and a focusing method⁴⁴ was used to optimize the boundary conditions of the grid. The charges on the C1' atoms of the DNA nucleosides were slightly modified in order for the bases to achieve electrical neutrality.²⁵ Likewise, the methylene C atoms joining the chromophores to the linking chains of ditercalinium and Flexi-Di were used as buffers to make the overall charge of chromophores and linkers equal to +1 or +2, respectively. The rest of the drug and DNA atoms were assigned the same charges and van der Waals radii that were employed in the molecular mechanics force field. Once this electrostatic interaction energy was characterized for a given pair of molecular fragments, it was possible to derive *effective dielectric constants*,⁴³ $\epsilon_e = E_{\text{el(MM)}}/E_{\text{el(PB)}}$, which were later used in the electrostatic energy analysis of the complexes during the molecular dynamics simulations.

The Poisson–Boltzmann equation was also used to calculate the electrostatic potential around the drug–d(CGCGCG)₂ complexes in order to find an optimal distribution for the explicit sodium ions included in the molecular dynamics simulations in water. To this end, the potential values at all points inside the volume occupied by the complex were set to zero, and a series of focused calculations allowed us, with the aid of the Insight II graphical interface, to place the counterions in a pairwise manner: the first two sodium ions were located in the vicinity of those areas yielding the most negative electrostatic potential; these two ions were explicitly included in the next calculation, which was corrected for the new ionic

strength, and helped locate the position of two more positive ions. This procedure was repeated as needed until electro-neutrality was achieved for each system, and each sodium ion replaced a water molecule from the equilibrated box of solvent. This novel method favored equilibration of the systems to a larger extent than other previously reported methods^{25,26} (data not shown) since the sodium ions were more effectively located in minimum energy configurations.

(3) Molecular Dynamics Simulations. Once the sodium ions were included, each solvated model system was relaxed as reported above. Molecular dynamics simulations then followed at 298 K and 1 atm using a nonbonded cutoff of 10 Å. Both the temperature and the pressure were weakly coupled to thermal and pressure baths⁴⁵ with relaxation times of 0.1 and 0.6 ps, respectively. In a 5-ps heating phase, the temperature was raised to 300 K in steps of 10 K over 0.1-ps blocks, and the velocities were reassigned at each new temperature according to a Maxwell–Boltzmann distribution. This was followed by an equilibration phase of 15 ps at 300 K, in which the velocities were reassigned in the same way every 0.2 ps during the first 5 ps, and by a 480-ps sampling period during which system coordinates were saved every 0.2 ps. The time step used was 1 fs during the heating period and 2 fs for the rest of the simulations. All bonds involving hydrogens were constrained to their equilibrium values by means of the SHAKE algorithm,³⁶ and the lists of nonbonded pairs were updated every 25 steps.

(4) Analysis of the Dynamics Trajectories. Interaction energies between the DNA molecule and each ligand, between parts of each ligand and parts of the DNA molecule, or between DNA subfragments, as well as several conformational parameters for both ligands and DNA molecules, were monitored and analyzed using the 2400 coordinate sets saved during the last 480 ps of the dynamics simulations. All of the molecular mechanics energy analyses were performed using a nonbonded cutoff of 10 Å and the estimated effective dielectric constants for the electrostatic interactions. Data smoothing for plotting purposes was accomplished by means of routine SMOOFT.⁴⁶ The conformational and helical parameters of the DNA tetramers and hexamers were analyzed by means of the program developed and kindly provided by Marla Babcock *et al.* at Rutgers University.⁴⁷

Results

Preliminary Calculations on the X-ray Crystallographic Structures. Figure 3 shows the X-ray crystal structures of the ditercalinium and Flexi-Di complexes displaying both the reported and energy optimized linkers. As mentioned above, optimization of the interactions involving the linkers prior to the molecular dynamics simulations was essential in order to obtain stable trajectories. In the ditercalinium complex, the modeled linker runs diagonally across the major groove in a more symmetrical fashion than in the reported structure, so that the Lennard–Jones and electrostatic interactions with the central bases are improved (Table 1). The Flexi-Di linker, with much larger intrinsic conformational variability (Figure 1b), also adapts better to the major groove in the refined complex (Figure 3) while the electrostatic interactions with the central bases are maintained, especially with the N7 atoms of the guanines. This attractive electrostatic component, which includes the hydrogen bonds deduced from the crystal structures, would account for the *pull* mechanism proposed to contribute to the DNA bending on the basis of specific hydrogen bonding interactions.²³ No reasons have been advanced, however, as to the origin of the proposed *push* emanating from interactions between the chromophores and the base pairs.

The interaction energy decomposition analyses performed on the X-ray crystallographic structures of

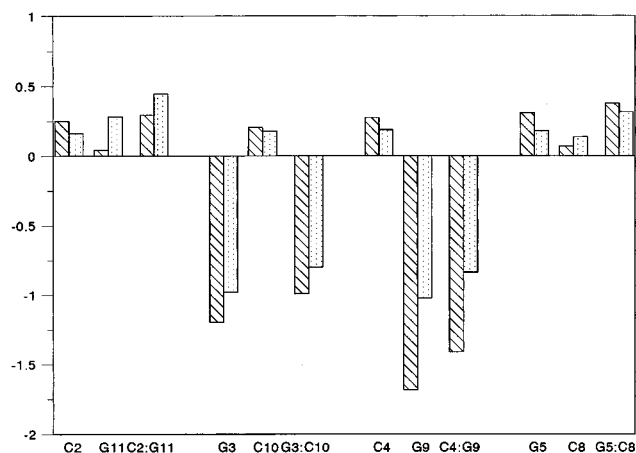


Figure 4. Solvent-screened electrostatic energy components (kcal mol^{-1}) of the stacking interactions between the 10-methoxy-7H-pyrido[4,3-c]carbazolium drug chromophores and either the central (G3:C10 and C4:G9) or the external (C2:G11 and G5:C8) base pairs in the X-ray crystal structures of ditercalinium–d(CGCG)₂ (hatched bars) and Flexi-Di–d(CGCG)₂ (dotted bars) complexes. Energy contributions are also given for each individual base. The C1' atoms of the nucleobases and the carbon attached to the quaternized nitrogen of the chromophores were used as buffers in order to achieve electrical neutrality or a total charge of +1, respectively.

d(CGCG)₂ complexed to either ditercalinium or Flexi-Di showed the Lennard–Jones term of the stacking energy to be very similar for the interactions between the drugs' chromophores and the DNA base pairs on each side of the intercalation sites. Neither adaptation of the structures to the AMBER force field nor refinement of the linkers brought about any significant differences (Table 1). On the contrary, analysis of the electrostatic contributions to the stacking energies between the 10-methoxy-7H-pyridocarbazolium rings and the DNA bases revealed this binding energy component to be *favorable* for the inner base pairs clamped by the chromophores (G3:C10 and C4:G9), but *unfavorable* for the base pairs that make up the boundaries of the bis-intercalation site (C2:G11 and G5:C8). When this favorable binding energy contribution was further decomposed in terms of the individual bases (Figure 4), the electrostatic interaction was found to be *attractive* for the internal guanines but *repulsive* for the internal cytosines. This discrimination can account for the experimentally observed poor van der Waals contacts of the chromophores with the internal cytosines.^{21–23} With regard to the electrostatic term of the stacking interaction between the chromophores and the bases that delimit the bis-intercalation sites, they are consistently *repulsive* in both crystal structures, which could account for the absence of van der Waals contacts with the external cytosines and for the observed bending of the helix.

The present results thus provide quantitative support to a qualitative description formulated earlier based on interpretation of the molecular electrostatic potentials (MEPs) of the stacked systems.⁴⁸ It was then pointed out that the graphical representation of the MEPs on a plane close to the recognition surface was very helpful in order to understand electrostatic complementarity and repulsive interactions. For a G:C pair, the most negative MEP region is found in the surroundings of the N7 and O6 atoms of guanine whereas the most

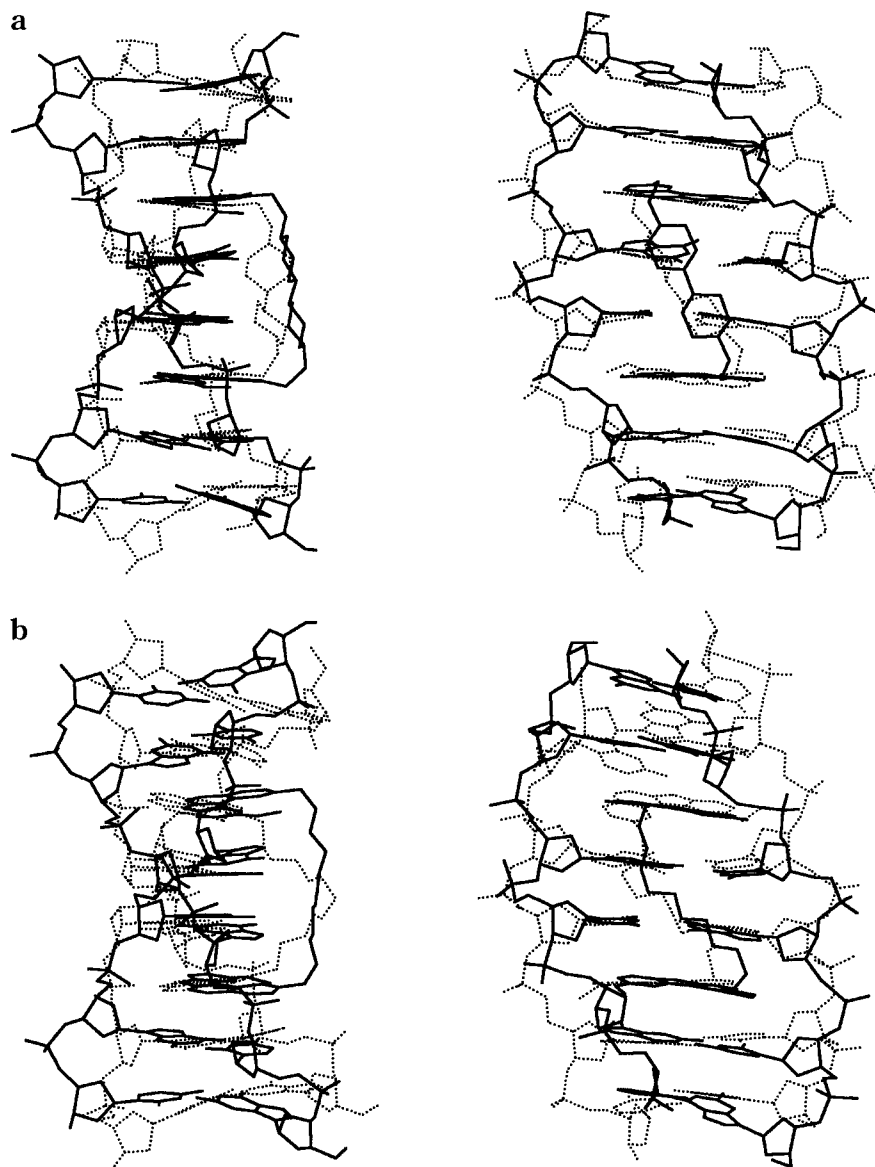


Figure 5. Side and front views of the energy-minimized average structures from the 400–500-ps period of the molecular dynamics simulations in water (dotted lines) superimposed on the initial refined models (thick lines) of $d(\text{GCGCGC})_2$ complexed to ditercalinium (a) and Flexi-Di (b).

positive MEP region is located around the cytosine ring (the resulting dipole moment for a G:C base pair in Watson–Crick conformation is about 5 Debye and the corresponding vector can be represented as an arrow pointing toward the cytosine base, as in Figure 2).²⁵ Since orientational preferences are known to be accentuated in steps involving G:C base pairs,^{18,25} the definite orientation of the 7*H*-pyridocarbazolium rings intercalated at the CpG steps and the distinct stacking features can thus be viewed as the result of concomitant optimization of the electrostatic attraction with the inner bases (G3:C10 and C4:G9, and particularly between the more positive ring A and the overlapping N7,-O6 region of guanine) and minimization of the electrostatic repulsion with C2:G11 and G5:C8, whose orientation relative to the drugs' chromophores is reversed (Figure 2). The AMBER force field is also sensitive to these differences, which are even more clearly marked (Table 1) upon careful energy refinement of the crystal structures and reoptimization of the linkers' geometries (Figure 3). Therefore, the chromophores of ditercalinium and Flexi-Di appear to act as very effective *clamps*

for the internal GpC step and, simultaneously, as *wedges* for the bases that form the boundary of the bis-intercalation site. In addition, the underwound central GpC step is also stabilized by stacking interactions relative to canonical A-type or B-type DNA (see below).

Molecular Dynamics Simulations of Ditercalinium- $d(\text{GCGCGC})_2$ and Flexi-Di- $d(\text{GCGCGC})_2$ Model Complexes. 1. General Structure of the Complexes. For the whole length of the simulations in water, both drugs remained inserted into the DNA with their chromophores fully intercalated at the CpG steps regardless of whether the linkers were (Figure 5) or were not charged (Figure 6). This highlights the stabilizing nature of stacking interactions involving DNA base pairs, which can be particularly strong for chromophores bearing a net positive charge and will be discussed later. A rough measure of the conformational changes undergone by the different complexes is provided by continuous monitoring of the rmsd from the initial structures (Supporting Information, item 5). The complex with ditercalinium appears as the most stable, with an average rmsd after 500 ps of about 2.5 Å

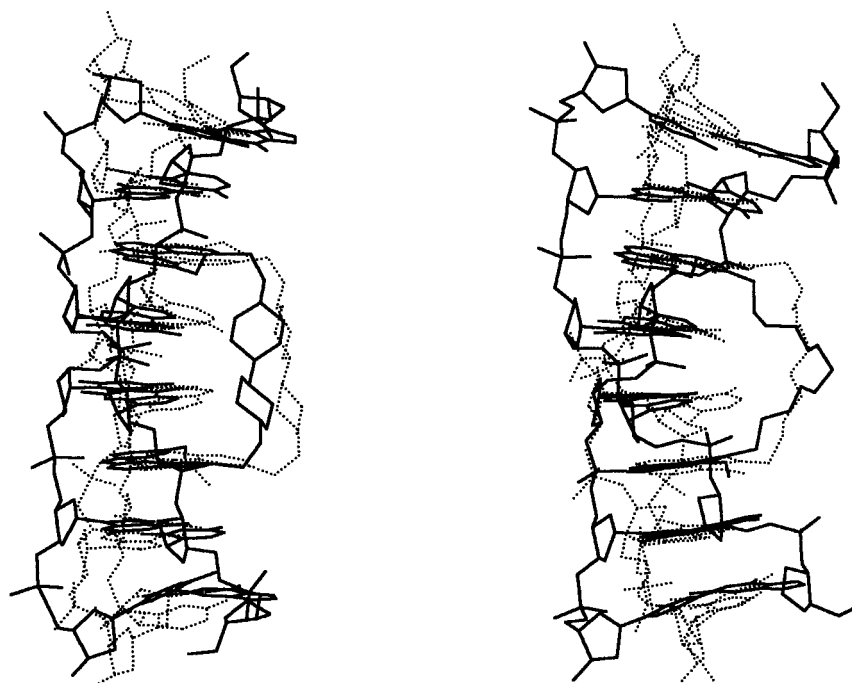


Figure 6. Side views of the energy-minimized average structures from the 400–500-ps period of the molecular dynamics simulations in water of $d(\text{CGCGCG})_2$ complexed to ditercalinium (left) and Flexi-Di (right), with charged (thick lines) or uncharged (dotted lines) linkers.

relative to the initial structure and of about 1 Å relative to the equilibrated structure in solution, whereas the complex with Flexi-Di is subject to slightly larger variations. The role of the linker in stabilization becomes clearer from comparison between complexes with charged and uncharged linkers. Since only the Lennard–Jones contribution is considered in these modified linkers, the effects due to electrostatics can be dissected out more easily, and these complexes are indeed shown to be the least stable of all (average rmsd values of about 3.5 and 4.5 Å for the ditercalinium and Flexi-Di complexes, respectively, at the end of the simulations).

2. Role of the Chains Connecting the Two Chromophores in Stability and Sequence Specificity. In the initial complexes, modeled on the X-ray crystal structures, the two protonated linker nitrogens of Flexi-Di form hydrogen bonds to N7 of residue G3 and to N7 and O6 of G9, whereas only one piperidinium nitrogen of ditercalinium is engaged in a hydrogen bond with N7 of residue G3 as the other one points toward the solvent. In our molecular dynamics simulations these hydrogen-bonding interactions soon compete with similar interactions with water, and the intermolecular hydrogen bonds initially present in the complexes are gradually lost during the first 50 ps of simulation to disappear completely during the next 150–300-ps sampling period. The ensuing conformational changes of the linkers contribute to the rmsd reported above, but the complexes remain stable nonetheless, as do the complexes in which the charges of the linkers were turned off. Therefore, other forces appear to be contributing to a large extent to the stability of the complexes in the absence of hydrogen bonds, and they will be discussed in the next subsection.

The higher degree of preorganization for bis-intercalation in ditercalinium vs Flexi-Di is manifested in the very different degrees of conformational variability

observed for the two molecules along the dynamics simulations, not only in the free state (data not shown) but also in their complexes with the DNA molecules. Conformational families were identified by dividing the conformational space of the linkers into hypercubes,⁴⁹ and assigning 0 (*anti*), + (*gauche* +), and – (*gauche* –) signs to each rotatable torsion angle. The last 100 ps of the simulations were used for comparison. Ditercalinium remained in the same hypercube (++–+–++) for virtually the whole length of the monitored simulation period; only a minor change in the second torsional angle (from + to 0) of the 7-torsion bis(piperidinium) linker (Figure 1a) was detected in one out of 500 frames. Ditercalinium has one of the piperidinium nitrogens oriented approximately toward the floor of the major groove and the other one pointing toward the solvent. Even though these groups definitely contribute to the electrostatic interaction energy, this does not necessarily mean that a hydrogen bond is established between the piperidinium nitrogen and the N7 or O6 atoms of the guanine opposite to it. This hydrogen bond was present in the initial structure and was seen during the first 50 ps of the simulation, but the optimal hydrogen-bonding geometry was lost thereafter due to competition with solvent molecules. When the charges of the linker were switched off, three hypercubes were found (++–00++, ++–+0++, and ++++0++), visited 434, 60, and 6 times, respectively, during the last 100-ps period. The relative increase in flexibility and the slightly different conformational preferences can thus be attributed to the loss of favorable electrostatic interactions between the linker and the central DNA base pairs, which is translated into decreased stability of the complex.

As expected, the number of hypercubes found for Flexi-Di both in the free state and in its complex with DNA was much larger than that found for ditercalinium. In the Flexi-Di–DNA complex, the 13-torsion

linker (Figure 1b) visited 24 hypercubes during the last 100 ps of the dynamics simulation in water (Supporting Information, item 6), with no clear preferences for one over another. Once again, hydrogen bonding of the protonated nitrogens to the major groove of the DNA competed with interactions with the water molecules, and the hydrogen bonds initially present between these nitrogens and the N7 and O6 atoms of the central guanines were not maintained. When the charges on the linker were switched off, both the type and the number of hypercubes visited changed, highlighting once again the dependence of torsional variability in the complex on electrostatic interactions with both the major groove and the solvent.

3. Stacking Interactions. The nature of the stacking interactions in these complexes has generally received little attention, but a more detailed analysis is necessary for a full understanding of the experimental data. The 10-methoxy-7*H*-pyrido[4,3-*c*]carbazolium chromophores contribute notably to the total interaction energies between these synthetic bifunctional intercalators and the DNA molecule. The Lennard–Jones and electrostatic contributions to the binding energy of these chromophores was shown in Table 1 for the crystal structures of the complexes. These contributions have also been monitored during the molecular dynamics simulations of the extended complexes in solution, both for the base pairs sandwiched by the chromophores and for the base pairs that form the boundary of the bis-intercalation site.

The Lennard–Jones contribution to the stacking energy remains virtually constant during the whole simulation with similar values for the interaction with the base pairs on either side of the intercalation sites (data not shown). In contrast, the electrostatic contributions, as was the case in the crystal structures of the complexes (Figure 4 and Table 1), are very different for each type of base pair and almost constantly remain *attractive* for the internal bases but *repulsive* for the external ones (Figure 7).

It is of interest to consider what happens at the DNA intercalation site itself. The central step comprising two G:C base pairs in antiparallel orientations is underwound relative to a standard DNA double helix, be it B-DNA or A-DNA (see next section). The sequence $d(\text{GCGCGC})_2$ has been reported not to crystallize under any of the many conditions surveyed, but on partial methylation of the cytosine residues, this alternating sequence has been shown to crystallize readily and to adopt a typical A-DNA conformation.⁵⁰ We have calculated the Lennard–Jones and electrostatic contributions to the stacking energy at a GpC step both in a canonical A-DNA conformation, as taken from fiber DNA diffraction data,⁵¹ and in the X-ray crystal structure of $d(\text{CCGGCGCCGG})_2$,³⁵ which crystallizes as B-DNA. These values range from -0.01 to -0.57 (electrostatic) and from -18.8 to -20.4 kcal mol⁻¹ (Lennard–Jones), in A- and B-DNA, respectively. The conformational energy change for the underwound central GpC step was then calculated as the difference in energy between the intercalated state along the dynamics trajectory and the standard A-DNA state (Supporting Information, item 7). The evolution of these energy differences (Lennard–Jones and electrostatic) along the

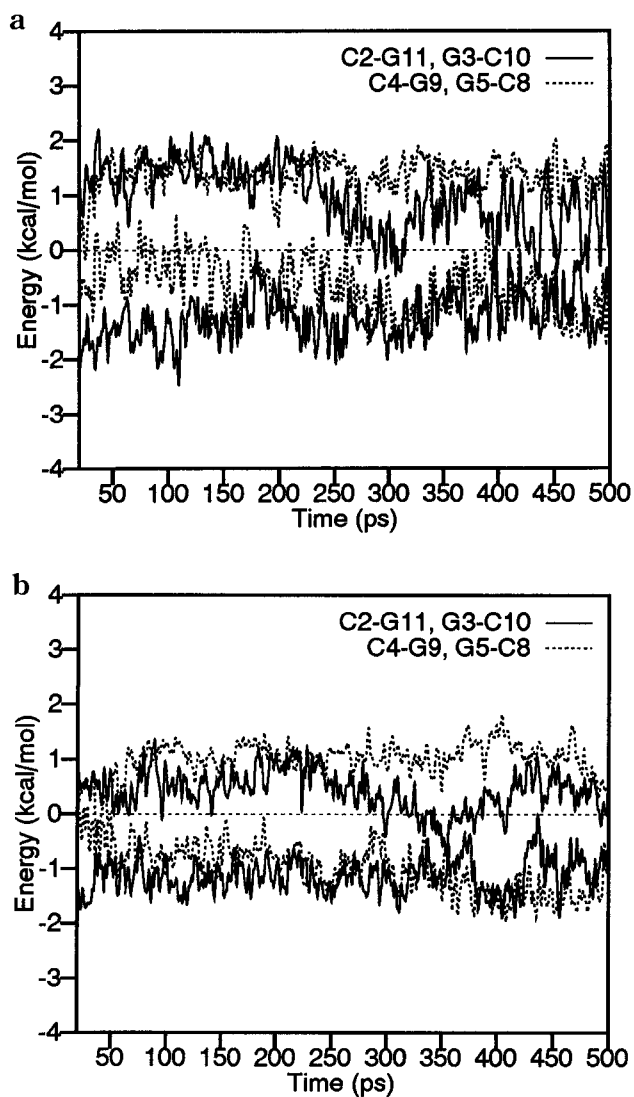


Figure 7. Electrostatic energy component (kcal mol⁻¹) of the stacking interaction between the chromophores of ditercalinium (a) or Flexi-Di (b) and either the sandwiched base pairs or the base pairs that form the boundary of the bis-intercalation site in their respective complexes with $d(\text{GCGCGC})_2$ along the molecular dynamics simulations. *Effective dielectric constants* of 9 and 5 were used for the interactions between the chromophores of ditercalinium and either the external (C2:G11 and G5:C8) or the central base pairs (G3:C10 and C4:G9, cf. Figure 2). The respective values for the Flexi-Di complex were 12 and 7.

dynamics simulations appears to indicate that, upon bis-intercalation, this step is *stabilized* relative to a GpC step in a standard DNA double helix. We suggest this favorable conformational energy change contributes to the binding energetics and may play an additional role in the sequence selectivity of this type of ligands.

4. DNA Conformation. Different conformational parameters of the DNA molecules were monitored⁴⁷ during the sampling period of the simulations (data not shown). In the following, we concentrate on three parameters that are especially relevant to the drug binding process and the subsequent conformational changes inflicted on the DNA molecule:⁵² the *rise* of each base pair along the helical axis, the *roll* angle between base pairs, and the *twist* of each base pair around the helical axis. Figure 8 shows the values of these parameters calculated for ditercalinium- $d(\text{CGCG})_2$ ^{21,22} and Flexi-Di- $d(\text{CGCG})_2$ ²³ crystal structures and for an

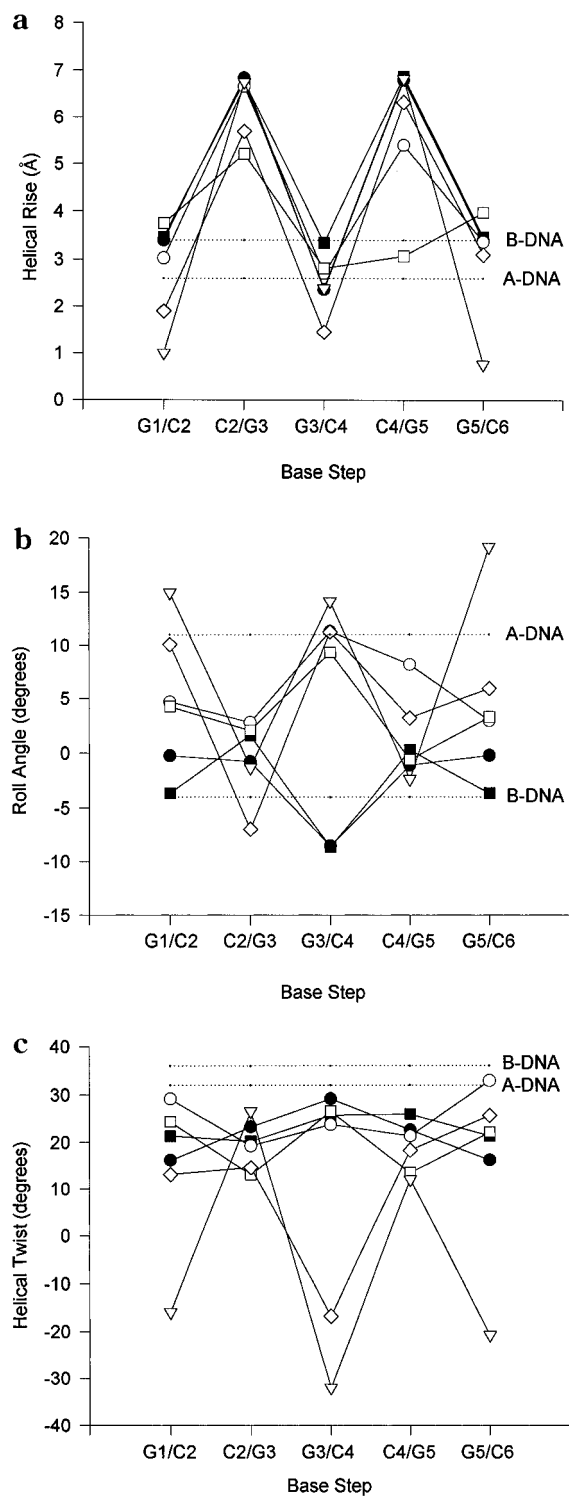


Figure 8. Helical rise (a), roll angle (b), and helical twist (c) parameters for every base pair step of the different complexes studied. Values for fiber A- and B-type DNA (dotted lines) are shown for comparison. The crystal structures of ditercalinium- $d(\text{CGCG})_2$ (filled circles) and Flexi-Di- $d(\text{CGCG})_2$ (filled squares) include on each side of the helix the extra base pair from a symmetry-related copy that was used in the modeling procedure. For the modeled complexes, the energy-minimized average structures from the 400–500-ps period of the molecular dynamics simulations in water were used: ditercalinium (open circles), Flexi-Di (open squares), ditercalinium with uncharged linker (diamonds), and Flexi-Di with uncharged linker (inverted triangles).

energy-minimized average structure representative of each modeled complex during the last 100 ps of the molecular dynamics simulations in water. For com-

parison, the reference values for a DNA double helix in either an A-type or a B-type conformation⁵¹ are also shown.

The *helical rise* in a standard A-DNA is 2.5 Å (Figure 8a), as opposed to 3.4 Å in B-DNA. The G3/C4 step sandwiched between the two chromophores of either ditercalinium or Flexi-Di presents values of 2.6 Å both in the crystal structures and in the average structure from the dynamics simulations of the extended complexes. Switching off the charges of the linker atoms causes a reduction in the magnitude of this parameter in this central region (1.5 Å). The base pairs separated by the intercalating chromophores (C2/G3 and C4/G5) provide rise values of 6.7 Å in the crystal structures that are maintained along the simulations except for the Flexi-Di–DNA complex and the ditercalinium complex without charges on the linker, where slightly smaller values were found (5–5.5 Å).

With regard to the rise of the external base pairs (G1/C2 and G5/C6 in Figure 8a), average values close to those of standard A-DNA were found along the dynamics simulations though they showed greater variability compared to the central base pairs due to fraying effects, which also affected the calculated time-dependent rmsd reported above.

Average *roll angles* measured for canonical A-DNA and B-DNA steps are around 11° and –4°, respectively. In the crystal structures of ditercalinium- and Flexi-Di-bound DNA, roll values of around –8° are found for the central step (G3/C4) and close to zero for the C2/G3 and C4/G5 steps that make up the intercalation sites for the drug chromophores (Figure 8b). In both cases, the value of this parameter reflects a B-like character of the complexed DNA which is rather different from the putative A-like character of its uncomplexed counterpart in the solid state. Interestingly, in our simulations we consistently find positive roll and negative slide values for the central G3/C4 step, which thus adopts features characteristic of A-DNA. These two conformational parameters have been recently shown to clearly separate A- and B-DNA helical families.⁵²

No major differences in roll were detected for C2/G3 and C4/G5 steps with respect to the crystal structures (Figure 8b). On the other hand, the terminal dimer steps (G1/C2 and G5/C6) display the low positive roll values characteristic of GpC steps in alternating d(GpC) hexamers,⁵⁰ which are intermediate between those of canonical A- and B-type DNAs. Thus, the change in roll is largely restricted to the central step, and the major consequence is that the distorted helix becomes more A-like.

The average *helical twist* angle in fiber A-DNA is about 32° vs 36° in canonical B-DNA.⁵¹ In the drug–DNA crystal complexes, both the steps making up the intercalation sites and the central steps are underwound, and the corresponding twist angles are maintained during the dynamics simulations. The average twist values are somewhat smaller for the C2/G3 and C4/G5 steps in the Flexi-Di complex and somewhat larger for the central step in the ditercalinium complex (Figure 8c). It is of interest that in the crystal structures of $d(\text{Gm}^5\text{CGm}^5\text{CGC})_2$ and $d(\text{Gm}^5\text{CGCG})_2$ the CpG steps have been shown to have lower than average twist angles (~29°).⁵⁰ The terminal dimer steps

(G1/C2 and G5/C6), which were added to the crystal structures of the drug–DNA complexes to extend the double helix and to minimize end effects, retain the twist angles (Figure 8c) characteristic of both fiber A-DNA and GpC steps in crystals of alternating dG–dC hexanucleotides.⁵⁰

In the simulations where the charges of the linkers were switched off, the helical twist was greatly reduced, especially at the central step. By comparing the 100-ps averaged structures, it appears that the DNA hexamers in these complexes are more unwound than the corresponding hexamers from the standard simulations (Figure 6), suggesting that the presence of positive charge in the major groove has a stabilizing effect on the DNA structure. That this is indeed the case is highlighted by monitoring the potential energy of the DNA molecules in the four complexes (Supporting Information, item 8): only in the simulations with charged linkers does the energy of the DNA remain virtually constant.

Discussion

The highly directional electrostatic component of the stacking interactions present in the X-ray crystal structures of ditercalinium–d(CGCG)₂^{21,22} and Flexi-Di–d(CGCG)₂²³ has been shown to provide *stabilization* between the drugs' chromophores and the central base pair step and *destabilization* between these same chromophores and the base pairs that form the boundary of the bis-intercalation site (Figure 4; Table 1). The model of like charges repelling one another and unlike charges attracting one another is also valid for molecules and molecular fragments, and the energy minimum found in the crystal structures can be thought of as the balance point of minimized repulsive and maximized attractive stacking interactions between electric quadrupole moments.⁵³ This stacking arrangement is sequence-dependent, and together with the favorable electrostatic attraction between the positively charged linkers and the negative major groove,⁵⁴ provides a theoretical basis for the preferred orientation of the chromophores and for the proposed "push/pull" effect²³ that may be responsible for the DNA curvature detected in these crystallographic structures. The chromophores of these drugs thus behave as very effective clamps for the sandwiched base pairs and have a "wedge" effect on the external bases, which are "pushed" into the minor groove.

The *shift* into the minor groove of the terminal bases, and the negative *roll* at the central base pair step (Figure 8a), observed in these structures can be viewed as one of the mechanisms by which these stacked heteroaromatic systems can accommodate repulsive and attractive interactions within the constraints imposed by the double helical structure and the presence of the linker.⁴⁸ On the other hand, it has been recognized that lattice contacts in the crystal may be selecting a conformation that is not predominant in solution, hence the desirability of studying complexes in different crystal forms and with longer DNA fragments.^{22,23} In the absence of additional crystallographic information, we have extended the calculations on the crystal complexes to model systems having an extra base pair on each side, and their behavior in solution has been simulated by means of molecular dynamics techniques.

The analyses of the resulting trajectories confirm the opposite electrostatic character of the stacking interactions calculated on each side of the intercalation site (Figure 7) and provide a rationale for the binding preferences of these drugs, which cannot be accounted for by hydrogen-bonding mechanisms. From the calculations presented in this paper, it would seem that the electrostatically directed preference of the 10-methoxy-7*H*-pyrido[4,3-*c*]carbazolium chromophore to stack in a definite orientation on a G:C base pair is playing a determinant role in both selecting a CpG step for intercalation and placing the linker in the major groove. Another specificity factor that is identified from the conformational analyses of the DNA molecules (Figure 8) is the naturally low twist angle exhibited by this particular step, both in A-DNA⁵⁰ and in B-DNA,⁵² which might be favoring intercalation. Moreover, once intercalation has taken place at both CpG steps, the sandwiched GpC step is *stabilized* relative to a GpC step in a standard DNA double helix. All of these factors combined make the alternating CpGpCpG sequence a particularly attractive target for ditercalinium and Flexi-Di binding.

The linkers alone appear unable to discriminate between GpC and CpG steps, since N7 and O6 atoms of guanines lie diagonally across the major groove in both steps. It seems highly unlikely that probes such as these can detect this base pair reversal. In the conformation displayed by these drugs in the crystal structures, stacking interactions with a central CpG step could be optimized only if the linker resides in the minor groove, where it would be disallowed by the exocyclic 2-amino group of the guanines. On the other hand, by rotation about the methylene bonds that join the linkers' protonated nitrogens to the chromophores, it should be possible for the drugs to adopt a Z-shape conformation, as opposed to the inverted Z-shape shown in Figure 2, which would in principle enable them to optimize both their stacking interactions with the base pairs and the electrostatic and dispersion interactions with the major groove of a CpG step. Since ditercalinium is known not to embrace the central CpG step when binding to d(GCGC)₂,¹¹ other factors must be at play, the most likely being the opposite conformational tendencies (*e.g.* twist) of GpC and CpG steps both in A-⁵⁰ and B-DNA,⁵² and differences in the energy needed to open up pyrimidine–purine compared to purine–pyrimidine steps.¹⁷

Our simulations suggest that the possible intermolecular hydrogen bonds between the linkers of the drugs and the major groove compete with similar interactions with the solvent. It thus seems that the electrostatic free energy loss associated with the removal of these protonated nitrogens and hydrogen-bonding acceptor groups from water cannot be compensated by the formation of the corresponding hydrogen bonds at the interface between the two interacting molecules.⁵⁵ As a matter of fact, comparison of the DNA binding properties of polyammonium ions and their peralkylated derivatives has shown that the contribution of hydrogen bonds to the binding affinity is indeed very small.⁵⁶ Our molecular dynamics results would further support the view⁵⁷ that polyamines bind to DNA in an essentially nonspecific manner through electrostatic rather than hydrogen-bonding interactions.

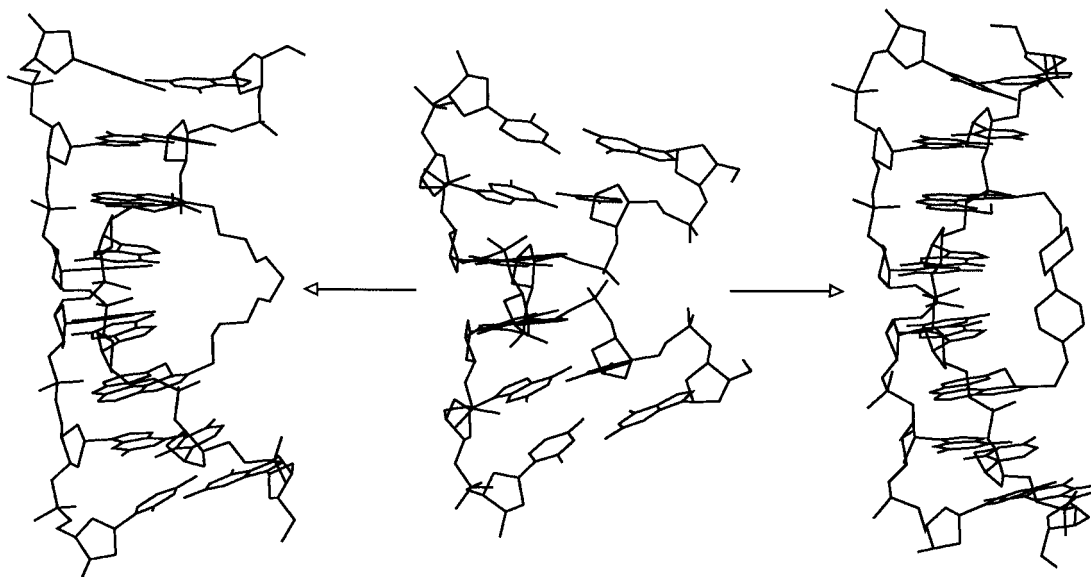


Figure 9. Structures of $d(\text{GCGCGC})_2$ in an ideal A-type conformation (middle) and in the complexes with Flexi-Di (left) or ditercalinium (right), as seen in the energy-minimized average structures from the 400–500-ps period of the molecular dynamics simulations in water.

The role of the linker in sequence discrimination would thus appear to vary greatly among different bis-intercalators. In the natural antibiotics triostin A or echinomycin, the two chromophores are attached to a depsipeptide, which establishes a number of hydrogen bonds with the DNA minor groove. These hydrogen bonds are effectively shielded from competitive interactions with the water molecules^{25,26} in a manner similar to what is observed in actinomycin D–DNA complexes.⁵⁸ For ditercalinium and Flexi-Di, this is clearly not the case, and the linkers of these molecules can be expected to contribute to the overall binding affinity but not to the sequence specificity. Moreover, as suggested above, the location of these linkers in the major groove would be the result of the marked electrostatically directed orientational preferences displayed by the quaternized 10-methoxy-7*H*-pyrido[4,3-*c*]carbazolium chromophores with regard to the highly polarized nucleobases.⁵⁹ Indirect support for this suggestion is provided by the nucleic acid stain TOTO,⁶⁰ which also binds to DNA through bis-intercalation, and displays high affinity for the sequence CTAG.⁶¹ Upon binding to this sequence, the rather bulky and charged tetramethylated diazaundecamethylene linker accommodates itself into the minor groove of the TpA step.²⁰ It has been proposed that the intrinsic twisted shape of TOTO's benzothiazolyl–methylidene–quinolinium chromophores must contribute to the sequence specificity by adapting easily to the characteristic propeller twist of the central TpA step.²⁰ The preferred orientation of the chromophores would then place in the minor groove the quaternized linker, which does not exhibit site selectivity by itself. Test MEP calculations in our group provide evidence that electrostatic stacking interactions are also optimized in this complex. Furthermore, selection by TOTO of CTAG as the preferred binding sequence might also be related to the facts that ApG, in common with CpG, is one of the DNA steps with the lowest average *twist* values in B-DNA,⁵² which presumably favors intercalation of the chromophores, and TpA, in common with GpC, is a naturally overwound step.⁵²

The ditercalinium–DNA complex is intrinsically asymmetric due to the asymmetry of the drug linker (Figure 1), which has the proton on each nitrogen pointing in opposite directions so that if one is directed toward the floor of the major groove the other one necessarily points toward the surrounding solvent (Figure 3). It has been proposed that the activity of this drug may be related to dynamic interconversion between conformers that are distinguished on the basis of the relative orientations of their piperidinium rings.⁶² The major conformation found along our dynamics simulation is actually an intermediate between these two possible conformers (Figure 5a), none of which appears to be particularly favored on the simulation time scale mainly due to competing interactions of both protonated nitrogens with the water molecules. For Flexi-Di, a wide range of conformations is available to the linker, which in principle could establish up to four hydrogen bonds with the major groove acceptor atoms.²³ However, in common with ditercalinium, the initial intermolecular hydrogen bonds are exchanged with similar interactions with the solvent.

In order to understand the conformational changes brought about by ditercalinium or Flexi-Di complexation, it is essential to consider the morphology of the DNA molecule prior to drug binding. Alternating dG–dC hexanucleotides incorporating methylated cytosine residues have been recently found to readily crystallize as A-DNA rather than Z-DNA at low salt concentrations provided the sequence motif be $d(\text{GCGCGC})$ as opposed to $d(\text{CGCGCG})$.⁵⁰ The fully unmethylated sequence was found not to crystallize under any conditions surveyed, but there were no noticeable effects of cytosine methylation on the helical parameters.⁵⁰ Therefore, the hexanucleotide studied here most likely adopts an A-type conformation (Figure 9) in the free state.

Compared to B-DNA, A-DNA has a wider minor groove, a narrower major groove, and a slightly smaller helical repeat (~ 11 base pairs per turn). In addition, the base pairs are not perpendicular to the helix axis ($\sim 18^\circ$ inclination) and are displaced away from the axis

and toward the major groove ($shift = -4.5 \text{ \AA}$). We have calculated the major conformational parameters for the drug–DNA complexes, both in the crystal structures and along the dynamics simulations in water, and compared them to those of fiber and crystal A- and B-type DNA molecules (Figure 8).

The DNA in the crystal complexes of d(CGCG)₂ with either ditercalinium or Flexi-Di is better described as B-DNA. The bending of the DNA double helix toward the minor groove is a consequence of the positive $shift$ ($\sim 2.6 \text{ \AA}$) and negative $roll$ (Figure 8b) at the central GpC step. These conformational parameters change for the hexanucleotide complexes along the dynamics simulations in water so that the DNA in the equilibrated complexes can be better described as A-DNA. One very distinct feature of these complexes, which can be discerned in the energy-optimized average structures from the last 100 ps of the simulations, is that the bending of the helix is not directed toward the minor groove, as it was in the starting conformations, but to the major groove instead (Figure 5). The changes in sign of the $roll$ values at the central GpC steps (Figure 8b) are mainly responsible for this reversal in the direction of bending and indicate that lattice contacts may be affecting the conformation of the DNA in the crystal complexes.

The feasibility of a model in which an A-type DNA structure, characterized by significant unwinding and a bend into the major groove, is stabilized by the noncovalent binding to the major groove of a positively charged bis-intercalating drug is supported by two independent lines of circumstantial evidence. First, the intrinsic curvature associated with the periodic distribution of dA_n tracts in kinetoplast DNA from *Crithidia fasciculata* has been shown to be completely removed by ditercalinium at saturating concentrations.⁶³ Since it was estimated that about one ditercalinium molecule is bound for each half-turn of the non- dA_n tracts at drug saturation, and unwinding of the helix (and the concomitant dephasing of the curved tracts) can only account for a small fraction of curving removal, the bending toward the major groove observed in the present work could provide a compensatory mechanism to cancel this deformation and produce overall straight DNA. Second, footprinting studies using DNase I and the same kinetoplast DNA in the presence of ditercalinium suggest that the hypersensitivity to cleavage observed for the dA_n tracts might be due to bending toward the major groove in addition to widening of the minor groove.¹

In this respect, it is of interest that histones and other DNA binding proteins with cationic surfaces can induce substantial DNA bending by neutralizing phosphates on one face of the DNA.⁶⁴ Likewise, DNA molecules partially modified by incorporation of neutral phosphate analogues are deformed toward the neutralized surface.⁶⁵ By adding positive charge to the face of the major groove of DNA (whose electrostatic potential is most negative in G:C regions),^{48,54} ditercalinium and Flexi-Di might be causing bending of DNA toward the major groove for similar reasons as histones do. However, the positive charge does not neutralize the phosphates selectively in these complexes, and in the simulations with neutralized linkers, a similar degree of bending

toward the major groove was observed (Figure 6). Our interpretation is that stacking interactions are at the origin of the bending, which can be modulated by factors such as the environment, helical constraints, and the presence of additional flanking bases. The electrostatic interactions between the linkers and the floor of the major groove, both of which compete with interactions with water, appear nevertheless to act in a concerted fashion with the stacking interactions to provide further stabilization to both the DNA (Supporting Information, items 5 and 8) and the complex (Table 1). Additionally, the intercalating moieties and the presence of the charged linkers in the major groove must have an influence on the scanning and processing abilities of different DNA-binding proteins.

As a matter of fact, ditercalinium-bound DNA is a target^{4,66} for enzymes involved in locating and repairing damaged sites within large domains of DNA, and particularly for the nucleotide excision repair system,⁶⁷ which recognizes a wide variety of lesions including cyclobutane pyrimidine dimers, benzo[*a*]pyrene–guanine adducts, thymine–psoralen adducts and guanine–cisplatin adducts,⁶⁸ all of which have been shown to induce curvature into the major groove.^{69–72} However, a kink is neither a sufficient nor a necessary determinant for damage recognition,^{67,68} and destabilization of the base-stacking interactions in the vicinity of the altered site has been singled out as the common feature of all DNA modifications that are recognized as damage by the excinuclease repair machinery.⁶⁸ The nature of this destabilization in ditercalinium– and Flexi-Di–DNA complexes has already been discussed.

Both ditercalinium and Flexi-Di promote binding of the excinuclease to undamaged DNA and stimulate its cleavage in *Escherichia coli*,^{4,66} which may trigger apoptosis.⁷³ Other noncovalent complexes between DNA and drugs such as ethidium, Hoechst 33258, or actinomycin D have also been shown to act as surrogate lesions in *E. coli* although the level of incision observed was comparatively smaller.⁷⁴ These drugs were also shown to be capable of inhibiting (A)BC excinuclease activity by forming ternary UvrA–drug–DNA complexes and to enhance incision at certain sites of UV photodamage.⁷⁴ It would be extremely interesting to know the extent and characteristics of DNA deformation in one of these ternary complexes where the binding interfaces might be partially or completely desolvated.

Ditercalinium, but not Flexi-Di, is endowed with antitumor properties. In eukaryotic cells, a delayed toxicity is observed, both *in vitro* and *in vivo*, at drug concentrations far below those required to observe immediate toxic effects. Ditercalinium is concentrated in mitochondria where DNA is rapidly and totally degraded. As a consequence, mitochondrial DNA-coded proteins are no longer synthesized, and the respiratory chain is progressively inactivated.⁷⁵ Human excinuclease is considerably more complex than *E. coli* (A)BC excinuclease, and the subunits comprising the two systems do not share any homology.⁶⁷ Since neither the crystal structures nor the results of our simulations provide any hints as to the origin of the distinct pharmacological profiles of these two bis-intercalating agents based on differential DNA deformation, the differences must be sought elsewhere. It is possible that

the conformationally more restricted bis(piperidinium) linker of ditercalinium is better suited for interacting with a particular protein of the eukaryotic repair machinery. In this respect, we note that the presence of a protonated ring nitrogen has been shown to be an essential requirement for the binding of other repair enzymes.⁷⁶

Conclusions

The main interactions present in the crystal complexes of ditercalinium and Flexi-Di with the alternating d(CGCG)₂ tetranucleotide have been analyzed in detail and compared to the interactions that take place along the molecular dynamics simulations of the complexes of these two drugs with d(GCGCGC)₂ in aqueous solution. A common energy component that contributes to complex stabilization is the *attractive* electrostatic stacking interaction between the drugs' chromophores and the base pairs sandwiched between them. In addition, the underwound central base pair step is stabilized relative to a standard GpC step.

The stacking specificities for the central GpC step are in concert with the attractive electrostatic interactions between the protonated nitrogens of the linkers and the N7 and O6 atoms of guanines which shape two regions of very negative electrostatic potential in the major groove.^{48,54} The summation of these effects is that the sandwiched base pairs are very effectively stapled by the drugs. The hydrogen-bonding potential of the linkers, however, would appear to be reduced in an aqueous medium due to competing interactions with water. This conclusion is further substantiated by results from simulations in which the charges of the linkers were "switched off".

These findings are in agreement with the observed preference of the chromophores of both ditercalinium and Flexi-Di to embrace a 5'-GpC-3' over a 5'-CpG-3' step¹¹ and give further support to the suggested relevance that stacking interactions may have in dictating or modulating sequence selectivity.²⁴ Intercalating chromophores should then be viewed not as simple hydrophobic plates that get sandwiched indiscriminately between the base pairs but as molecular fragments endowed with significant electric quadrupole moments and marked orientational preferences. They can thus behave as additional elements of binding specificity by taking advantage of the distinct electrostatic properties of G:C and A:T base pairs.⁴⁸

On the other hand, the electrostatic interactions between the pyridocarbazole chromophores and the base pairs that delimit the bis-intercalation site are *repulsive* and may be largely responsible for the notable structural features reported for these complexes in the solid state.²¹⁻²³ The structural effects on the external bases appear to depend on the environment, helical constraints, and the presence of additional flanking bases. Our molecular dynamics results with the hexanucleotide d(GCGCGC)₂ suggest that ditercalinium and Flexi-Di may stabilize an A-type DNA conformation in solution characterized by significant unwinding and a bend into the major groove. Interestingly, these structural features are probably already present in the free oligonucleotide.⁵⁰

The remarkable similarities between the complexes of d(CGCG)₂ with either ditercalinium or Flexi-Di and

that of TOTO with d(CTAG)₂ suggest that selection of the binding sequence by these bis-intercalating ligands, whose linkers span diagonally the DNA grooves (major or minor), may be dictated by optimization of the interactions with the central step, the nature of the adjacent bases being largely determined by the ease of unwinding in order to allow intercalation of the chromophores.

Acknowledgment. Financial support from the Spanish Ministerio de Educación y Ciencia (B.P.T. and J.G.) and Comunidad Autónoma de Madrid (A.R.O.) is gratefully acknowledged. This research has been financed in part by the Spanish Comisión Interministerial de Ciencia y Tecnología (SAF94/0630). The University of Alcalá provided a generous grant of SG Power Challenge computer time. Biosym Technologies, Inc. (San Diego, CA) contributed a software license.

Supporting Information Available: AMBER parameters and partial atomic charges for ditercalinium and Flexi-Di and four additional figures (8 pages). Ordering information is given on any current masthead page.

References

- (1) Mendoza, R.; Markovits, J.; Jaffrezou, J.-P.; Muzard, G.; Le Pecq, J.-B. Dnase I Susceptibility of Bent DNA and Its Alteration by Ditercalinium and Distamycin. *Biochemistry* **1990**, *29*, 5035-5043.
- (2) Pelaprat, D.; Delbarre, A.; Le Guen, I.; Roques, B. P. DNA Intercalating Compounds as Potential Antitumor Agents. 2. Preparation and Properties of 7H-Pyridocarbazole Dimers. *J. Med. Chem.* **1980**, *23*, 1336-1343.
- (3) Delbarre, A.; Delepierre, M.; Garbay, C.; Igolen, J.; Le Pecq, J.-B.; Roques, B. P. Geometry of the Antitumor Drug Ditercalinium Bisintercalated into d(CpGpCpG)₂ by ¹H NMR. *Proc. Natl. Acad. Sci. U.S.A.* **1987**, *84*, 2155-2159.
- (4) Lambert, B.; Roques, B. P.; Le Pecq, J.-B. Induction of an Abortive and Futile DNA Repair Process in *E. coli* by the Antitumor DNA Bifunctional Intercalator, Ditercalinium: Role of *polA* in Death Induction. *Nucleic Acid Res.* **1988**, *16*, 1063-1078.
- (5) Delepierre, M.; Maroun, R.; Garbay-Jaureguiberry, C.; Igolen, J.; Roques, B. P. ¹H- and ³¹P Nuclear Magnetic Resonance Studies of the Differences in DNA Deformation Induced by Antitumoral 7H-pyrido[4,3-c]carbazole Dimers. *J. Mol. Biol.* **1989**, *210*, 211-228.
- (6) Pothier, J.; Delepierre, M.; Barsi, M.-C.; Garbay-Jaureguiberry, C.; Igolen, J.; Le Bret, M.; Roques, B. P. Comparison of the Bis-intercalating Complexes Formed Between Either Ditercalinium or a Flexible Analogue and d(CpGpCpG)₂ or d(TpTpCpGpCpGpA)₂ Minihelices: ¹H- and ³¹P-NMR Analyses. *Biopolymers* **1991**, *31*, 1309-1323.
- (7) Léon, P.; Garbay-Jaureguiberry, C.; Lambert, B.; Le Pecq, J. B.; Roques, B. P. Asymmetrical Bisintercalators as Potential Antitumor Agents. *J. Med. Chem.* **1988**, *31*, 1021-1026.
- (8) Léon, P.; Garbay-Jaureguiberry, C.; Le Pecq, J. B.; Roques, B. P. Relationship Between the Size and Position of Substituents on 7H-Pyrido[4,3-c]Carbazole Monomers and Dimers and their DNA Binding and Anti-tumor Properties. *Anticancer Drug Des.* **1988**, *3*, 1-13.
- (9) (a) Delbarre, A.; Delepierre, M.; Igolen, J.; Le Pecq, J. B.; Roques, B. P. ¹H NMR Studies of the Structure of a Pyridocarbazole Dimer-d(CpGpCpG) Complex. *Biochimie* **1985**, *67*, 823-828. (b) Delbarre, A.; Delepierre, M.; D'Estaintot, B. L.; Igolen, J.; Roques, B. P. Bisintercalation of Ditercalinium into a d(CpGpCpG)₂ Minihelix: Structure and Dynamics Aspects - A 400-MHz ¹H-NMR Study. *Biopolymers* **1987**, *26*, 1001-1033.
- (10) Delepierre, M.; Igolen, J.; Roques, B. P. Study of the Bisintercalation of the Antitumor Drug Ditercalinium by ³¹P-NMR. *Biopolymers* **1988**, *27*, 957-968.
- (11) Delepierre, M.; Milhe, C.; Namane, A.; Dinh, T. H.; Roques, B. P. ¹H- and ³¹P-NMR Studies of Ditercalinium Binding to a d(GCGC)₂ and d(CCTATAGG)₂ Minihelices: A Sequence Specificity Study. *Biopolymers* **1991**, *31*, 331-353.
- (12) Sobell, H. M.; Jain, S. C. Stereochemistry of Actinomycin Binding to DNA. II. Detailed Molecular Model of Actinomycin-DNA Complex and its Implications. *J. Mol. Biol.* **1972**, *68*, 21-34.
- (13) Krugh, T. R. Drug-DNA Interactions. *Curr. Opin. Struct. Biol.* **1994**, *4*, 351-364.

- (14) Müller, W.; Crothers, D. M. Interactions of Heteroaromatic Compounds with Nucleic Acids. 1. Influence of Heteroatoms and Polarizability on the Base Specificity of Intercalating Ligands. *Eur. J. Biochem.* **1975**, *54*, 267–277.
- (15) Krugh, T. R.; Reinhardt, C. G. Evidence for Sequence Preferences in the Intercalative Binding of Ethidium Bromide to Dinucleoside Monophosphates. *J. Mol. Biol.* **1975**, *97*, 133–162.
- (16) Day, R. O.; Seeman, N. C.; Rosenberg, J. M.; Rich, A. A Crystalline Fragment of the Double Helix: The Structure of the Dinucleoside Phosphate Guanylyl-3',5'-Cytidine. *Proc. Natl. Acad. Sci. U.S.A.* **1973**, *70*, 849–853.
- (17) Nuss, M. E.; Marsh, F. J.; Kollman, P. A. Theoretical Studies of Drug-Dinucleotide Interactions. Empirical Energy Function Calculations on the Interaction of Ethidium, 9-Aminoacridine, and Proflavin Cations with the Base-Paired Dinucleotides GpC and CpG. *J. Am. Chem. Soc.* **1979**, *101*, 825–833.
- (18) Ornstein, R. L.; Rein, R.; Breen, D. L.; MacElroy, R. D. An Optimized Potential Function for the Calculation of Nucleic Acid Interaction Energies. I. Base Stacking. *Biopolymers* **1978**, *17*, 2341–2360.
- (19) Pindur, U.; Haber, M.; Sattler, K. Antitumor Active Drugs as Intercalators of Deoxyribonucleic Acid. Molecular Models of Intercalation Complexes. *J. Chem. Educ.* **1993**, *70*, 263–272 and references cited therein.
- (20) Spielmann, H. P.; Wemmer, D. E.; Jacobsen, J. P. Solution Structure of a DNA Complex with the Fluorescent Bis-intercalator TOTO Determined by NMR Spectroscopy. *Biochemistry* **1995**, *34*, 8542–8553.
- (21) Gao, Q.; Williams, L. D.; Egli, M.; Rabinovich, D.; Chen, S. L.; Quigley, G. J.; Rich, A. Drug-Induced DNA Repair: X-ray Structure of a DNA-Ditercalinium Complex. *Proc. Natl. Acad. Sci. U.S.A.* **1991**, *88*, 2422–2426.
- (22) Williams, L. D.; Gao, Q. DNA-Ditercalinium Interactions: Implications for Recognition of Damaged DNA. *Biochemistry* **1992**, *31*, 4315–4324.
- (23) Peek, M. E.; Lipscomb, L. A.; Bertrand, J. A.; Gao, Q.; Roques, B. P.; Garbay-Jaureguiberry, C.; Williams, L. D. DNA Distortion in Bis-Intercalated Complexes. *Biochemistry* **1994**, *33*, 3794–3800.
- (24) Gallego, J.; Luque, F. J.; Orozco, M.; Burgos, C.; Alvarez-Builla, J.; Rodrigo, M. M.; Gago, F. DNA Sequence-Specific Reading by Echinomycin: Role of Hydrogen Bonding and Stacking Interactions. *J. Med. Chem.* **1994**, *37*, 1602–1609.
- (25) Gallego, J.; Ortiz, A. R.; Gago, F. A Molecular Dynamics Study of the Bis-intercalation Complexes of Echinomycin with d(ACGT)₂ and d(TCGA)₂: Rationale for Sequence-Specific Hoogsteen Base-Pairing. *J. Med. Chem.* **1993**, *36*, 1548–1561.
- (26) Gallego, J.; Luque, F. J.; Orozco, M.; Gago, F. Binding of Echinomycin to d(GCGG)₂ and d(CCGG)₂: Distinct Stacking Interactions Dictate the Sequence-Dependent Formation of Hoogsteen Base Pairs. *J. Biomol. Struct. Dyn.* **1994**, *12*, 111–129.
- (27) Bernstein, F. C.; Koetzle, T. F.; Williams, G. J. B.; Meyer, E. F., Jr.; Brice, M. D.; Rodgers, J. R.; Kennard, O.; Shimanouchi, T.; Tasumi, M. The Protein Data Bank: A Computer-based Archival File for Macromolecular Structures. *J. Mol. Biol.* **1977**, *112*, 535–542.
- (28) Gago, F.; Reynolds, C.; Richards, W. G. The Binding of Nonintercalative Drugs to Alternating DNA Sequences. *Mol. Pharmacol.* **1989**, *35*, 232–241.
- (29) Pearlman, D. A.; Case, D. A.; Caldwell, J.; Seibel, G.; Singh, U. C.; Weiner, P.; Kollman, P. A. AMBER version 4.0 1991. Department of Pharmaceutical Chemistry, University of California, San Francisco.
- (30) Weiner, S. J.; Kollman, P. A.; Nguyen, D. T.; Case, D. A. An All Atom Force Field for Simulations of Proteins and Nucleic Acids. *J. Comput. Chem.* **1986**, *7*, 230–252.
- (31) Hopfinger, A. J.; Pearlstein, R. A. Molecular Mechanics Force-field Parameterization Procedures. *J. Comput. Chem.* **1984**, *5*, 486–499.
- (32) Singh, U. C.; Kollman, P. A. An Approach to Computing Electrostatic Charges for Molecules. *J. Comput. Chem.* **1984**, *5*, 129.
- (33) Besler, B. H.; Merz, K. M., Jr.; Kollman, P. A. Atomic Charges Derived from Semiempirical Methods. *J. Comput. Chem.* **1990**, *11*, 431–439.
- (34) Goodsell, D. S.; Kopka, M. L.; Dickerson, R. E. Refinement of Netropsin Bound to DNA: Bias and Feedback in Electron Density Map Interpretation. *Biochemistry* **1995**, *34*, 4983–4993.
- (35) Heinemann, U.; Alings, C. The Conformation of a B-DNA Decamer is Mainly Determined by its Sequence and Not by Crystal Environment. *EMBO J.* **1991**, *10*, 35–43.
- (36) Ryckaert, J. P.; Ciccotti, G.; Berendsen, H. J. C. Numerical Integration of the Cartesian Equations of Motion of a System with Constraints: Molecular Dynamics of n-alkanes. *J. Comput. Phys.* **1977**, *23*, 327–341.
- (37) Jorgensen, W. L.; Chandrasekhar, J.; Madura, J. D. Comparison of Simple Potential Functions for Simulating Liquid Water. *J. Chem. Phys.* **1983**, *79*, 926–935.
- (38) Aqvist, J. Ion-Water Interaction Potentials Derived from Free Energy Perturbation Simulations. *J. Phys. Chem.* **1990**, *94*, 8021–8024.
- (39) Jayaram, B.; Sharp, K. A.; Honig, B. The Electrostatic Potential of DNA. *Biopolymers* **1989**, *28*, 975–993.
- (40) Klapper, I.; Hagstrom, R.; Fine, R.; Sharp, K.; Honig, B. Focusing of Electric Fields in the Active Site of Cu-Zn Superoxide Dismutase: Effects of Ionic Strength and Amino-acid Modification. *Proteins* **1986**, *1*, 47–59.
- (41) Insight-II, version 2.2.0 (1994). Biosym Technologies Inc., 9685 Scranton Rd, San Diego, CA 92121–2777.
- (42) Lee, B.; Richards, F. M. The Interpretation of Protein Structure: Estimation of Static Accessibility. *J. Mol. Biol.* **1971**, *55*, 379–400.
- (43) Friedman, R. A.; Honig, B. The Electrostatic Contribution to DNA Base-Stacking Interactions. *Biopolymers* **1992**, *32*, 145–159.
- (44) Gilson, M. K.; Sharp, K. A.; Honig, B. H. Calculating the Electrostatic Potential of Molecules in Solution: Method and Error Assessment. *J. Comput. Chem.* **1988**, *9*, 327–335.
- (45) Berendsen, H. J. C.; Postma, J. P. M.; van Gusteren, W. F.; DiNola, A.; Haak, J. R. Molecular Dynamics with Coupling to an External Bath. *J. Chem. Phys.* **1984**, *81*, 3684–3690.
- (46) Press, W. H.; Flannery, B. P.; Teukolsky, S. A.; Vetterling, W. T. In *Numerical Recipes*; Cambridge University Press: Cambridge, UK, 1989.
- (47) Babcock, M. S.; Pednault, E. P. D.; Olson, W. K. Nucleic Acid Structure Analysis: Mathematics for Local Cartesian Helical Structure Parameters that are Truly Comparable Between Structures. *J. Mol. Biol.* **1994**, *237*, 125–156.
- (48) Gallego, J.; de Pascual-Teresa, B.; Ortiz, A. R.; Pisabarro, M. T.; Gago, F. Molecular Electrostatic Potentials of DNA Base Pairs and Drug Chromophores in Relation to DNA Conformation and Bis-Intercalation by Quinoxaline Antibiotics and Ditercalinium. In *QSAR and Molecular Modelling: Concepts, Computational Tools and Biological Applications*; Sanz, F., Giraldo, J., Manaut, F., Eds.; J. R. Prous: Barcelona, Spain, 1995; pp 274–281.
- (49) Bruccoleri, R. E.; Karplus, M. Conformational Sampling Using High-Temperature Molecular Dynamics. *Biopolymers* **1990**, *29*, 1847–1862.
- (50) Mooers, B. H. M.; Schoth, G. P.; Baxter, W. W.; Ho, P. S. Alternating and Non-alternating dG-dC Hexanucleotides Crystallize as Canonical A-DNA. *J. Mol. Biol.* **1995**, *249*, 772–784.
- (51) Arnott, C. F.; Hukins, D. W. Optimised Parameters for A-DNA and B-DNA. *Biochem. Biophys. Res. Commun.* **1972**, *47*, 1504–1509.
- (52) Gorin, A. A.; Zhurkin, V. B.; Olson, W. K. B-DNA Twisting Correlates with Base-pair Morphology. *J. Mol. Biol.* **1995**, *247*, 34–48.
- (53) Williams, J. H. The Molecular Electric Quadrupole Moment and Solid-State Architecture. *Acc. Chem. Res.* **1993**, *26*, 593–598.
- (54) Lavery, R.; Pullman, B. The Dependence of the Surface Electrostatic Potential of B-DNA on Environmental Factors. *J. Biomol. Struct. Dyn.* **1985**, *2*, 1021–1032.
- (55) Honig, B.; Nicholls, A. Classical Electrostatics in Biology and Chemistry. *Science* **1995**, *268*, 1144–1149.
- (56) Schneider, H.-J., & Blatter, T. Interactions Between Acyclic and Cyclic Peralkylammonium Compounds and DNA. *Angew. Chem., Int. Ed. Engl.* **1992**, *31*, 1207–1208.
- (57) Cullis, P. M.; Merson-Davies, L.; Weaver, R. Conjugation of a Polyamine to the Bifunctional Alkylating Agent Chlorambucil Does Not Alter the Preferred Cross-Linking Site in Duplex DNA. *J. Am. Chem. Soc.* **1995**, *117*, 8033–8034.
- (58) Gallego, J.; Ortiz, A. R.; de Pascual-Teresa, B.; Gago, F. Unpublished results.
- (59) Rein, R. Studies of Biomolecular Interactions: Principles of Nucleic Acid Structure and Function from the Point of View of Constituent Interactions. In *Perspectives in Quantum Chemistry and Biochemistry*; Pullman, B., Ed.; John Wiley & Sons: New York, 1978; Vol. II, pp 307–362.
- (60) Rye, H. S.; Yue, S.; Wemmer, D. E.; Quesada, M. A.; Haugland, R. P.; Mathies, R. A.; Glazer, A. N. Stable Fluorescent Complexes of Double-stranded DNA with Bis-intercalating Asymmetric Cyanine Dyes: Properties and Applications. *Nucleic Acids Res.* **1992**, *20*, 2803–2812.
- (61) Jacobsen, J. P.; Pedersen, J. B.; Hansen, L. F.; Wemmer, D. E. Site Selective Bis-intercalation of a Homodimeric Thiazole Orange Dye in DNA Oligonucleotides. *Nucleic Acids Res.* **1995**, *23*, 753–760.
- (62) Peek, M. E.; Lipscomb, L. A.; Haseltine, J.; Gao, Q.; Roques, B. P.; Garbay-Jaureguiberry, C.; Williams, L. D. Asymmetry and Dynamics in Bis-intercalated DNA. *Bioorg. Med. Chem.* **1995**, *3*, 693–699.
- (63) Barceló, F.; Muzard, G.; Mendoza, R.; Révet, B.; Roques, B. P.; Le Pecq, J.-B. Removal of DNA Curving by DNA Ligands: Gel Electrophoresis Study. *Biochemistry* **1991**, *30*, 4863–4873.
- (64) Crothers, D. M. Upsetting the Balance of Forces in DNA. *Science* **1994**, *266*, 1819–1820.

- (65) Strauss, J. K.; Maher, L. J. DNA Bending by Asymmetric Phosphate Neutralization. *Science* **1994**, *266*, 1829–1834.
- (66) (a) Lambert, B.; Jones, B. K.; Roques, B. P.; Le Pecq, J. B.; Yeung, A. T. The Noncovalent Complex Between DNA and the Bifunctional Intercalator Ditercalinium is a Substrate for the UvrABC Endonuclease of *Escherichia coli*. *Proc. Natl. Acad. Sci. U.S.A.* **1989**, *86*, 6557–6561. (b) Lambert, B.; Segal-Bendirdjian, E.; Esnault, C.; Le Pecq, J. B.; Roques, B. P.; Jones, B.; Yeung, A. T. Recognition by the DNA Repair System of DNA Structural Alterations Induced by Reversible Drug-DNA Interactions. *Anticancer Drug Des.* **1990**, *5*, 43–53.
- (67) Sancar, A. Mechanisms of DNA Excision Repair. *Science* **1994**, *266*, 1954–1956.
- (68) Van Houten, B.; Snowden, A. Mechanism of Action of the *Escherichia coli* UvrABC Nuclease: Clues to the Damage Recognition Problem. *BioEssays* **1993**, *15*, 51–59.
- (69) Husain, I.; Griffith, J.; Sancar, A. Thymine Dimers Bend DNA. *Proc. Natl. Acad. Sci. U.S.A.* **1988**, *85*, 2558–2562.
- (70) Pearlman, D. A.; Holbrook, S. R.; Pirkle, D. H.; Kim, S.-H. Molecular Models for DNA Damaged by Photoreaction. *Science* **1985**, *227*, 1304–1308.
- (71) Tomic, M. T.; Wemmer, D. E.; Kim, S.-H. Structure of a Psoralen Cross-Linked DNA in Solution by Nuclear Magnetic Resonance. *Science* **1987**, *238*, 1722–1725.
- (72) Herman, F.; Kozelka, J.; Stoven, V.; Guittet, E.; Girault, J.-P.; Huynh-Dinh, T.; Igolen, J.; Lallemand, J.-Y.; Chottard, J.-C. A d(GpG)-Platinated Decanucleotide Duplex is Kinked. *Eur. J. Biochem.* **1990**, *194*, 119–133.
- (73) Martin, S. J.; Green, D. R.; Cotter, T. G. Dicing with Death: Dissecting the Components of the Apoptosis Machinery. *Trends Biochem. Sci.* **1994**, *19*, 26–30.
- (74) Selby C. P.; Sancar A. Noncovalent Drug-DNA Binding Interactions That Inhibit and Stimulate (A)BC Excinuclease. *Biochemistry* **1991**, *30*, 3841–3849.
- (75) (a) Segal-Bendirdjian, E.; Coulaud, D.; Roques, B. P.; Le Pecq, J. B. Selective Loss of Mitochondrial DNA after Treatment of Cells with Ditercalinium (NSC 335153), an Antitumor Bis-Intercalating Agent. *Cancer Res.* **1988**, *48*, 4982–4992. (b) Esnault, C.; Brown, S. C.; Segal-Bendirdjian, E.; Coulaud, D.; Mishal, Z.; Roques, B. P.; Le Pecq, J. B. Selective Alteration of Mitochondrial Function by Ditercalinium (NSC 335153), a DNA Bisintercalating Agent. *Biochem. Pharmacol.* **1990**, *39*, 109–122.
- (76) Schärer, O. D.; Ortholand, J.-Y.; Ganesan, A.; Ezaz-Nikpay, K.; Verdine, G. L. Specific Binding of the DNA Repair Enzyme AlkA to a Pyrrolidine-Based Inhibitor. *J. Am. Chem. Soc.* **1995**, *117*, 6623–6624.

JM9604179